Efficacy of FGFR Inhibitors and Combination Therapies for Acquired Resistance in FGFR2-Fusion Cholangiocarcinoma

Melanie A. Krook[1], Alexandria Lenyo[1], Max Wilberding[1], Hannah Barker[1], Mikayla Dantuono[1], Kelly M. Bailey[2], Hui-Zi Chen[1,3], Julie W. Reeser[1], Michele R. Wing[1], Jharna Miya[1], Eric Samorodnitsky[1], Amy M. Smith[1], Thuy Dao[1], Dorrelyn M. Martin[1], Kristen K. Ciombor[4], John Hays[1,5], Aharon G. Freud[1,6], and Sameek Roychowdhury[1,5]

ABSTRACT

The fibroblast growth factor receptor (FGFR) signaling pathway is aberrantly activated in approximately 15% to 20% of patients with intrahepatic cholangiocarcinoma. Currently, several FGFR kinase inhibitors are being assessed in clinical trials for patients with FGFR-altered cholangiocarcinoma. Despite evidence of initial responses and disease control, virtually all patients eventually develop acquired resistance. Thus, there is a critical need for the development of innovative therapeutic strategies to overcome acquired drug resistance. Here, we present findings from a patient with FGFR2-altered metastatic cholangiocarcinoma who enrolled in a phase II clinical trial of the FGFR inhibitor, infigratinib (BGJ398). Treatment was initially effective as demonstrated by imaging and tumor marker response; however, after 8 months on trial, the patient exhibited tumor regrowth and disease progression. Targeted sequencing of tumor DNA after disease progression revealed the *FGFR2* kinase domain p.E565A and p.L617M single-nucleotide variants (SNV) hypothesized to drive acquired resistance to infigratinib. The sensitivities of these *FGFR2* SNVs, which were detected post-infigratinib therapy, were extended to include clinically relevant FGFR inhibitors, including AZD4547, erdafitinib (JNJ-42756493), dovitinib, ponatinib, and TAS120, and were evaluated *in vitro*. Through a proteomics approach, we identified upregulation of the PI3K/AKT/mTOR signaling pathway in cells harboring the *FGFR2* p.E565A mutation and demonstrated that combination therapy strategies with FGFR and mTOR inhibitors may be used to overcome resistance to FGFR inhibition, specific to infigratinib. Collectively, these studies support the development of novel combination therapeutic strategies in addition to the next generation of FGFR inhibitors to overcome acquired resistance in patients.

Introduction

Cholangiocarcinoma is an aggressive tumor originating from the bile ducts. Unfortunately, most patients present with advanced stage disease, thus preventing curative therapy (1). For the limited number of patients who do present with resectable disease, survival rates remain low due to tumor recurrence. Five-year overall survival rates for patients with advanced stage disease have remained at less than 2% (1, 2). Because of poor prognosis and limited treatment options beyond chemotherapy and radiation, novel therapeutic strategies are needed for the treatment of cholangiocarcinoma. FGFR is aberrantly activated in approximately 15%–20% of intrahepatic cholangiocarcinomas and FGFR has emerged as an effective therapeutic strategy benefiting up to 70%–80% of patients harboring these alterations (3–6).

FGFRs are a family of receptors that control critical physiologic processes including cell proliferation, survival, growth arrest, differentiation, migration, and apoptosis (7). Deregulation and hyperactivation of the FGFR signaling cascade have been reported across many tumor types including urothelial carcinoma, intrahepatic cholangiocarcinoma, breast carcinoma, non–small cell lung carcinoma, endometrial carcinoma, and head and neck squamous cell carcinoma (8). Deregulation of FGFR occurs through various genomic alterations including gene fusions, single-nucleotide variants, alternative splicing, and copy number amplifications (9–11). Multiple FGFR tyrosine kinase inhibitors (TKI) have demonstrated clinical efficacy in patients with advanced FGFR-mutant cancers (12). Recently, erdafitinib received FDA approval for use in patients with FGFR-altered urothelial cancers. However, as seen with other targeted therapies, patients inevitably develop acquired resistance (13–15). Recent studies have identified the emergence of recurrent secondary single-nucleotide variants (SNV) in FGFR following FGFR inhibition that desensitize tumor cells to these therapies (16, 17). Therefore, there is a critical need to develop innovative therapeutic strategies, including novel FGFR inhibitors and combination therapies, to overcome acquired resistance in these patients.

In this study, we present a patient with *FGFR2* fusion–positive cholangiocarcinoma who initially responded to the FGFR inhibitor infigratinib but eventually developed disease progression. From tumor sequencing at the time of progression, we identified two acquired secondary *FGFR2* kinase domain mutations, p.E565A and p.L617M, which were hypothesized to drive acquired resistance to infigratinib.

[1]Comprehensive Cancer Center, The Ohio State University, Columbus, Ohio. [2]Department of Pediatrics, University of Pittsburgh School of Medicine, Pittsburgh, Pennsylvania. [3]Department of Internal Medicine, Hematology and Oncology Fellowship Program, The Ohio State University, Columbus, Ohio. [4]Division of Hematology and Oncology, Department of Medicine, Vanderbilt University Medical Center, Nashville, Tennessee. [5]Division of Medical Oncology, Department of Internal Medicine, The Ohio State University, Columbus, Ohio. [6]Department of Pathology, The Ohio State University, Columbus, Ohio.

Note: Supplementary data for this article are available at Molecular Cancer Therapeutics Online (http://mct.aacrjournals.org/).

Corresponding Author: Sameek Roychowdhury, The Ohio State University, 460 West 12th Avenue, Biomedical Research Tower, Room 996, Columbus, OH 43210. Phone: 614-685-5842; Fax: 614-292-6356; E-mail: sameek.roychowdhury@osumc.edu

Mol Cancer Ther 2020;19:847–57

doi: 10.1158/1535-7163.MCT-19-0631

Moreover, we confirmed this hypothesis through *in vitro* drug sensitivity studies utilizing cell lines transduced to stably express these *FGFR2* mutants. Through a proteomics approach, we identified upregulation of the PI3K/AKT/mTOR signaling pathway in cells expressing *FGFR2* p.E565A and further tested the effects of mTOR inhibitors, which resensitized these cells to FGFR inhibition. In summary, understanding how secondary mutations in FGFR affect sensitivity to different FGFR inhibitors and developing rational combination therapies will both be critical to improving the clinical outcome of patients with FGFR-altered cancers.

Materials and Methods

Patient

The patient provided informed written consent to an IRB-approved study entitled "Precision Cancer Medicine for Advanced Cancer Through High-throughput Sequencing" (NCT02090530) at The Ohio State University Comprehensive Cancer Center (Columbus, OH). This study allows for collection of fresh-frozen tumor biopsy, blood, serum, and buccal swab for multiplatform molecular characterization. Molecular diagnostic testing of pre- and posttreatment biopsies included a targeted RNA-based next-generation sequencing assay to detect gene fusions (OSU–SpARKFuse; ref. 18) and a targeted DNA sequencing assay to detect SNVs and copy number alterations as described previously (19). Sequencing data presented in the study have been submitted to dbGaP (https://ncbi.nlm.nih.gov/gap) under the project accession number phs001924.v1.p1.

Cell culture

NIH3T3 cells and HEK 293T cells were purchased from ATCC, and MMNK-1 cells were purchased from Japanese Collection of Research Bioresources Cell Bank (JCRB Cell Bank). NIH3T3 cells were cultured in DMEM (Life Technologies) supplemented with 10% bovine calf serum (ATCC). HEK 293T cells were cultured in DMEM (Life Technologies) supplemented with 10% Tet System Approved Fetal Bovine Serum (Takara). MMNK-1 cells were cultured in DMEM supplemented with 5% nonheat-inactivated FBS. All cells were incubated in a humidified incubator at 37°C with 5% CO_2. Short-tandem repeat profiling (20) and *Mycoplasma* testing (e-Myco plus Mycoplasma PCR Detection Kit, Bulldog Bio) were performed routinely to confirm identities and ensure cells were *Mycoplasma*-negative, respectively.

Fusion and secondary mutation generation

The *FGFR2-KIAA1598* gene fusion sequence was generated and cloned into the pLVX-IRES-Puro Vector (Clontech) by GenScript (Supplementary Text 1). GenScript used site-directed mutagenesis to introduce the *FGFR2* p.E565A and *FGFR2* p.L617M SNVs into the fusion. NIH3T3, 293T, and MMNK-1 cells were stably transduced with either empty, *FGFR2-KIAA1598* WT or *FGFR2-KIAA1598* p.E565A, or *FGFR2-KIAA1598* p.L617M lentiviral vectors and were subsequently selected and maintained in 1 μg/mL puromycin (Sigma) containing media prior to downstream applications. The presence of the fusion and mutations was confirmed by PCR and Sanger Sequencing as described previously (The Ohio State University Comprehensive Cancer Center Genomics Shared Resource, Columbus, OH; ref. 21). Primer sequences are listed in Supplementary Table S1.

Drug sensitivity assays

NIH3T3 and 293T cells were plated at 10,000 cells per well and MMNK-1 were plated at 5,000 cells per well in a 96-well plate and allowed to adhere for 24 hours. Cells were dosed with varying concentrations (0.01 to 5000 nmol/L) of FGFR inhibitors and allowed to incubate for 72 hours. FGFR inhibitors tested included infigratinib, AZD4547 (22), erdafitinib, TAS120 (23), dovitinib, and ponatinib (Cayman Chemical). Quantification of viability was carried out with the CellTiter 96 Aqueous Non-Radioactive Cell Proliferation Assay (Promega) per the manufacturer's protocol. The IC_{50} was calculated using GraphPad Prism. Four independent replicate experiments were conducted.

Reverse phase protein array

Cell pellets were submitted to The University of Texas MD Anderson Cancer Center (Houston, TX) and reverse phase protein array (RPPA) was performed as described previously (https://www.mdanderson.org/research/research-resources/core-facilities/functional-proteomics-rppa-core.html). Each condition was run in duplicate and GraphPad Prism was used to analyze the data. STRING (24) was used to determine protein–protein interactions from RPPA data.

Combination drug assays

NIH3T3 cells were plated at 10,000 cells per well in a 96-well plate. Twenty-four hours after plating, duplicate cells were exposed to either drug A, drug B, drug A plus drug B, or no drug control (**Fig. 4A**). We performed a nonconstant ratio combination of drugs A and B ranging from 6.85 nmol/L to 555 nmol/L (concentrations based on single-drug sensitivity assays). Drugs tested included the mTOR inhibitor, INK128 (25) in combination with an FGFR inhibitor (infigratinib, AZD4547, erdafitinib, TAS120, dovitinib, or ponatinib). After 72 hours, cell viability was assessed using the CellTiter 96 Aqueous Non-Radioactive Cell Proliferation Assay (Promega). Data from four independent experiments were compiled, and CalcuSyn (26) was used to calculate combination indexes (CI).

Western blotting

Western blot assays of whole-cell lysates were performed as described previously (27). We used the following antibodies: phospho-Akt (Ser473) #9271 (Cell Signaling Technology), Akt #9272 (Cell Signaling Technology), phospho-S6 ribosomal protein (Ser240/244) #2215 (Cell Signaling Technology), S6 ribosomal protein #2217 (Cell Signaling Technology), phospho-mTOR (Ser2448) #5536 (Cell Signaling Technology), mTOR #2983 (Cell Signaling Technology), and GAPDH sc27758 (Santa Cruz Biotechnology).

Immunofluorescence

A total of 15,000 cells were seeded into four-chamber polystyrene CultureSlides (BD Falcon) and allowed to adhere and spread for 12 hours. Cells were then fixed using 2% paraformaldehyde/PBS for 30 minutes at room temperature. Cells were washed three times with PBS and then permeabilized using 0.2% triton x-100/PBS for 10 minutes at room temperature. Blocking was performed using 5% FBS/PBS at room temperature for 30 minutes. Cells were stained for actin using Alexa Flour 488–conjugated phalloidin (Molecular Probes) and cortactin using 566-conjugated anti-cortactin clone 4F11 (EMD Millipore). Cells were again washed three times with 1× PBS and were mounted using and ProLong Gold Antifade Reagent with DAPI (Cell Signaling Technology). Stained cells were imaged using a Zeiss LSM 710 confocal microscope with a 63× oil objective. Images were analyzed using Zeiss software.

Results

Acquired resistance to infigratinib in a patient with FGFR2 fusion–positive cholangiocarcinoma

A 49-year-old female presented with a persistent cough, fatigue, chills, smell aversions, anorexia, diarrhea, weight loss, and epigastric pain. A CT scan showed subcentimeter pulmonary nodules and numerous large, poorly defined, enhancing, low-attenuation masses in the liver. Tissue biopsy of a liver lesion demonstrated metastatic intrahepatic cholangiocarcinoma. The patient was subsequently started on gemcitabine/cisplatin chemotherapy, but was intolerant of this regimen. XELOX chemotherapy (capecitabine/oxaliplatin) was initiated and continued for 4 months until, unfortunately, she developed progressive disease as indicated by CT scans. She underwent an ultrasound-guided tumor biopsy and next-generation sequencing (NGS) revealed an *FGFR2-KIAA1598* gene fusion (**Fig. 1A**). The fusion involved exons 1–17 of *FGFR2* and exons 8–18 of *KIAA1598* (also known as *SHTN1*; **Fig. 1B**). She was subsequently enrolled on the phase II multicenter, single-arm study of oral infigratinib in adult patients with advanced or metastatic cholangiocarcinoma with FGFR2 gene fusions or other FGFR genetic alterations who failed or are intolerant to platinum-based chemotherapy (NCT02150967). Per trial protocol, she received 125 mg of infigratinib daily orally (3 weeks on, 1 week off in a cycle). Over the course of the treatment, she underwent two dose reductions of infigratinib due to hyperphosphatemia (100 mg and 75 mg, respectively). CT scans indicated a partial response by RECIST criteria after 4 months of treatment along with decreases in CA 19–9 levels (**Fig. 1A**). After 8 months on study, the patient exhibited disease progression by CT scans per RECIST criteria, and treatment was discontinued (**Fig. 1A**). A repeat biopsy of progressive tumor revealed the same *FGFR2-KIAA1598* gene fusion; however, a SNV p.E565A was detected in the FGFR2 kinase domain (**Fig. 1A** and **C**). The patient received 1 dose of irinotecan (180 mg/m^2) followed by 1 dose of fluorouracil (5FU) + irinotecan (2,000 mg/m^2 and 150 mg/m^2). The irinotecan was reduced because of cytopenia. Unfortunately, due to progressive decline the patient then entered hospice care and passed away shortly thereafter. We also analyzed pre-(infigratinib) treatment and postprogression cell-free circulating tumor DNA (ctDNA) for SNVs using a targeted in-house DNA sequencing assay. Analysis of the postprogression ctDNA sample revealed a p.L617M mutation in addition to the p.E565A mutation that was present in the biopsy. Both of these mutations were detected exclusively in the postprogression ctDNA sample and not in the pretreatment ctDNA sample (**Fig. 1A**). The p.L617M mutation was not detected in the postprogression tumor biopsy sample demonstrating the limitations of tumor biopsies in capturing tumor heterogeneity.

In vitro characterization of the FGFR2–KIAA1598 fusion

We next sought to characterize the fusion and the secondary SNVs (p.E565A and p.L617M) through *in vitro* assays. We generated NIH3T3, 293T, and MMNK-1 cells expressing the control vector (empty), the wild-type *FGFR2-KIAA1598* fusion protein (FK WT), and the fusion protein containing either the p.E565A (FK p.E565A) or p.L617M (FK p.L617M) mutation. NIH3T3 and 293T cells were chosen as they do not express endogenous FGFR and therefore are ideal cell lines to study the functional contribution of the fusion and secondary mutations. MMNK-1 cells which are highly differentiated immortalized human cholangiocytes were also used to represent the cell of origin for cholangiocarcinoma (28). Successful transduction of NIH3T3, 293T, and MMNK-1 cells with empty vector, FK WT, FK p.E565A, or FK L617M was confirmed with PCR using primers that were designed to flank the fusion breakpoint (Supplementary Fig. S1A). Sanger sequencing also confirmed the fusion sequence and the p.E565A and p.L617M mutations (Supplementary Fig. S1B).

Given that the *KIAA1598* gene (also known as Shootin-1) has been shown to play a critical role in cytoskeletal organization (29), we were interested in whether the presence of the fusion impacted cellular morphology. We stained empty, FK WT, FK p.E565A, FK p.L617M containing NIH3T3, 293T, and MMMK-1 cells for actin, cortactin, and DAPI to visualize the cell cytoskeleton, including actin-based cell extensions and lamellipodia (**Fig. 2**). Interestingly, all of the cell lines containing the fusion (FK WT) and the fusion plus mutations (FK p.E565A and FK p.L617M) demonstrated dramatically different morphologies at baseline (**Fig. 2**). We noted that these cells were not able to spread as well, as demonstrated by decreased cell size and more elongated cellular morphology (**Fig. 2**). In addition, in the 293T and MMNK-1 cells we observed that the cells harboring the fusion exhibited decreased clustering compared with control cells, as demonstrated by more single, independent cells present in culture (**Fig. 2**). These findings suggest that the fusion disrupts both cell–cell contacts and cell–matrix contacts in cells.

Characterizing the sensitivity of secondary FGFR2 resistance mutations to various FGFR inhibitors

To evaluate the underlying mechanism of acquired resistance to FGFR inhibition in our patient, we evaluated the *in vitro* sensitivity of NIH3T3, 293T, and MMNK-1 cells expressing empty control, FK WT, FK p.E565A, and FK p.L617M cells to infigratinib. Cells were treated with increasing doses of infigratinib or DMSO (vehicle) ranging from 0.1 nmol/L to 20 μmol/L for 72 hours, at which point cell viability was assessed. The FK cells were particularly sensitive to infigratinib with an IC_{50} value of 18.24 nmol/L, whereas the FK p.E565A and FK p.L617M cells were resistant to infigratinib with IC_{50} values of 490.91 nmol/L and 2296.15 nmol/L, respectively (**Table 1**; Supplementary Fig. S2). The presence of the p.E565A and p.L617M mutations decreased the respective sensitivity to infigratinib by 27- and 126-fold (**Table 1**; Supplementary Fig. S2). These findings were also extended and corroborated in 293T and MMNK-1 cells, although MMNK-1 cells displayed weaker sensitivity overall (**Table 1**; Supplementary Fig. S2). Collectively, these *in vitro* findings support the clinical findings seen in this patient in that the FGFR2–KIAA1598 fusion is sensitive to infigratinib and that acquisition of the secondary kinase mutations, p.E565A and p.L617M, in part, drive resistance to infigratinib.

We next sought to assess the cross-reactivity of the fusion and the secondary SNVs to other FGFR inhibitors. We assessed several TKIs: AZD4547, erdafitinib, TAS120, dovitinib, and ponatinib. These inhibitors that are currently being evaluated clinically and have shown early efficacy in patients with FGFR-mutant cancers. NIH3T3, 293T, and MMNK-1 cells expressing the fusion were all sensitive to the selective FGFR inhibitors AZD-4547 and erdafitinib, the irreversible FGFR inhibitor TAS120, and the nonselective FGFR inhibitor ponatinib (**Table 1**; Supplementary Fig. S2). However, cells harboring either secondary mutation (FK p.E565A or FK p.L617M), were less sensitive to AZD-4547, erdafitinib, and TAS120, thus confirming the acquisition of these mutations as drivers of resistance to FGFR inhibition (**Table 1**; Supplementary Fig. S2). None of the cells were sensitive to dovitinib, a nonspecific TKI (**Table 1**; Supplementary Fig. S2). Interestingly, the FK-expressing cells and cells expressing FK p.E565A or FK p.L617M demonstrated equal sensitivity to the nonselective FGFR inhibitor ponatinib. These findings support further studies to determine whether ponatinib can be used clinically to overcome resistance

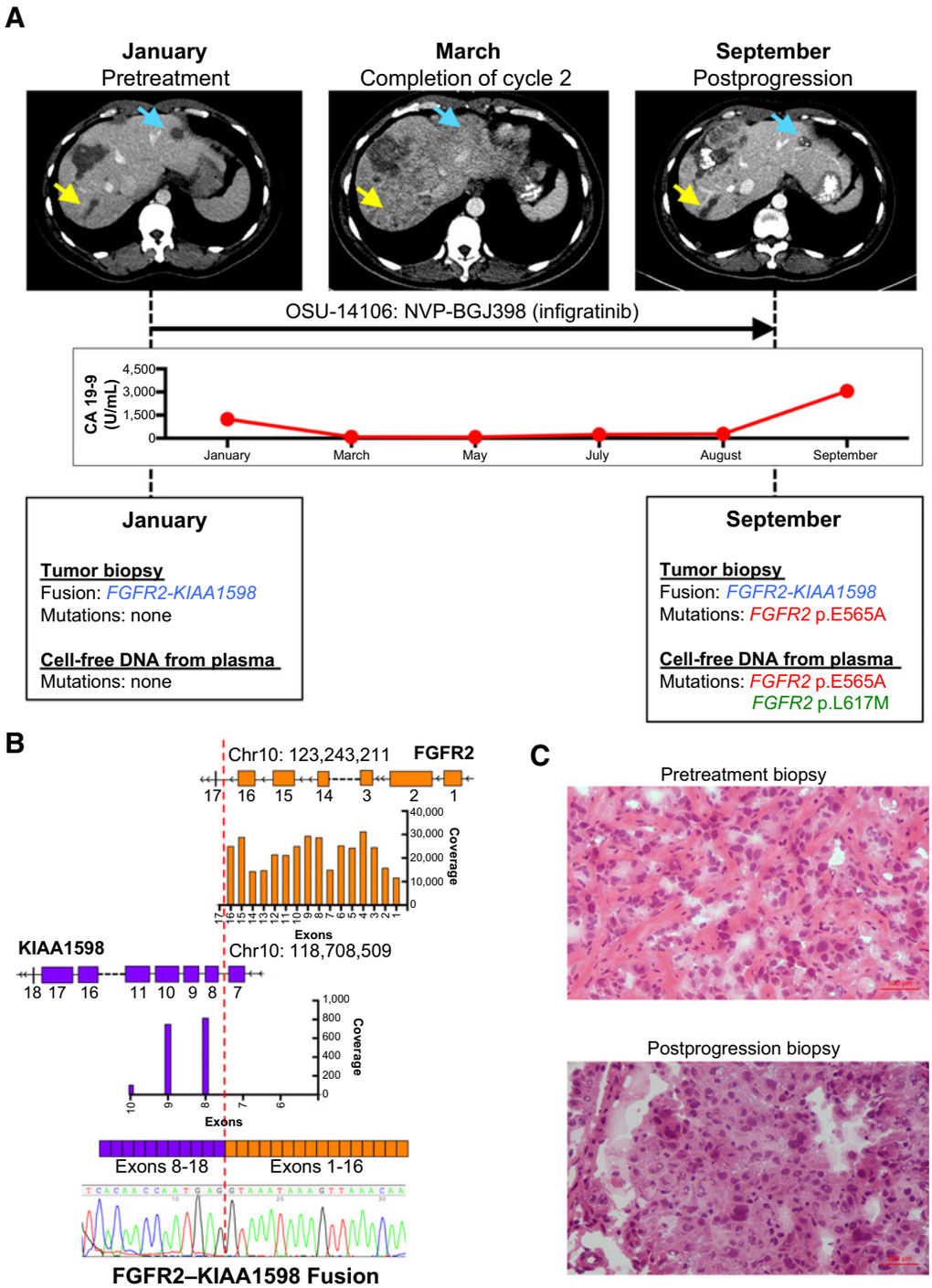

Figure 1.

Detection of a clinically actionable *FGFR2* fusion and two acquired secondary *FGFR2* mutations. **A,** A patient with metastatic cholangiocarcinoma who failed prior gemcitabine-based chemotherapy had a liver biopsy, and sequencing revealed an *FGFR2-KIAA1598* gene fusion. She was enrolled in a phase II clinical trial for the oral FGFR inhibitor, infigratinib, and had radiographic response after 2 months on therapy (yellow and blue arrows). After 8 months on therapy, she developed progression and underwent a repeat tumor biopsy. Sequencing revealed a secondary mutation, p.E565A, in the kinase domain of *FGFR2*. Sequencing of pretreatment and posttreatment ctDNA from plasma revealed the presence of the p.E565A and p.L617M SNVs in the *FGFR2* kinase domain present exclusively in the posttreatment samples. **B,** Schematic of the *FGFR2-KIAA1598* fusion gene containing exons 1–16 of *FGFR2* and exons 8–18 of *KIAA1598*. Chromatogram traces confirmed the presence of the fusion. The red dashed line indicates the breakpoint. **C,** Hematoxylin and eosin staining of the pretreatment and postprogression tumor biopsies demonstrate the abundance of tumor cells.

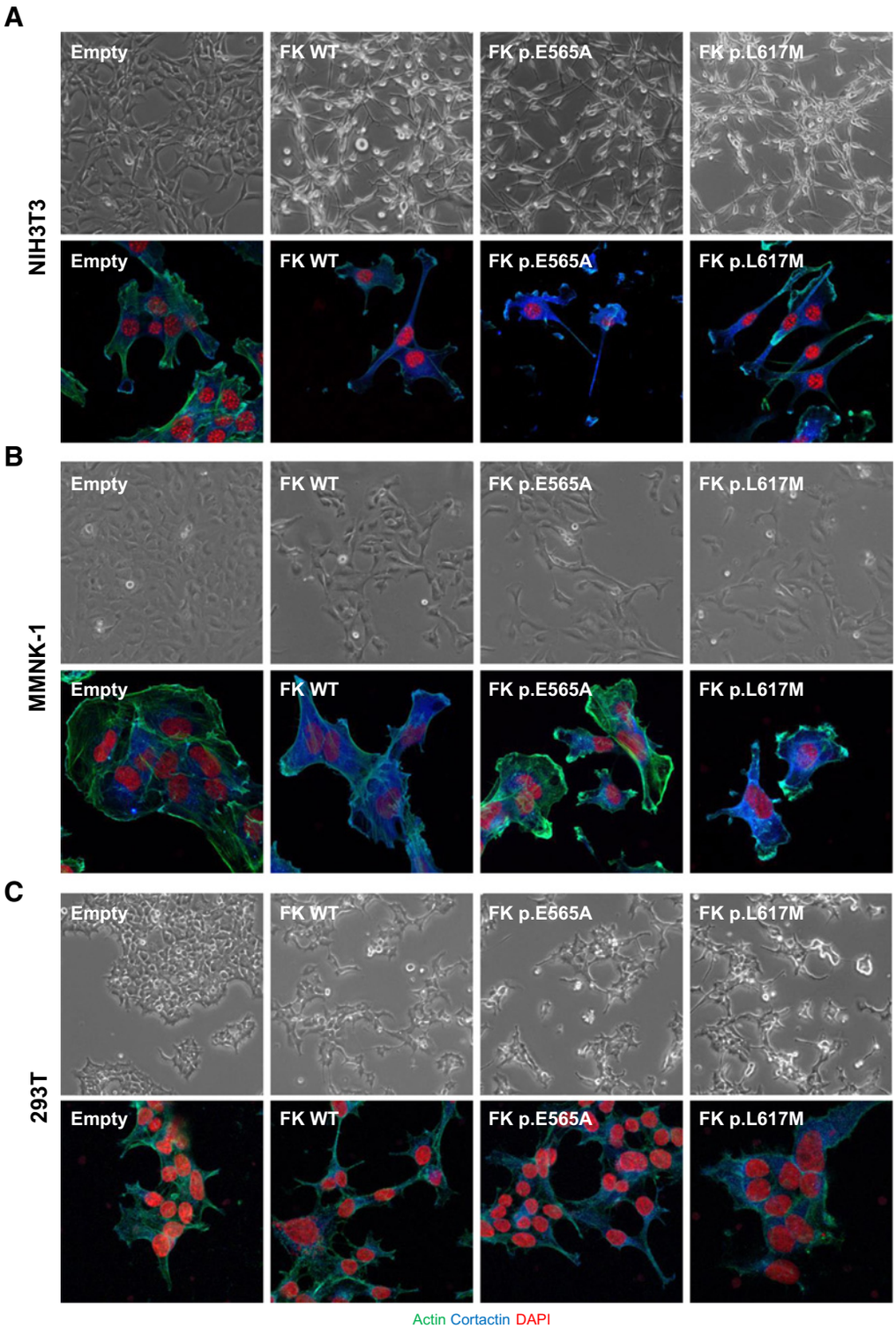

Figure 2.

The *FGFR2–KIAA1598* fusion induces morphologic changes. Fixed NIH3T3 (**A**), MMNK-1 (**B**), and 293T (**C**) cells expressing the fusion (FK) or the fusion with a secondary mutation (FK p.E565A and FK p.L617M) were stained with actin (green), cortactin (blue), and DAPI (red) to visualize differences in cell morphology.

Table 1. The *FGFR2* p.E565A and p.L617M mutations confer resistance to infigratinib and other FGFR inhibitors.

		IC_{50} (nmol/L) values					
		Infigratinib	**AZD4547**	**Erdafitinib**	**TAS120**	**Ponatinib**	**Dovitinib**
NIH3T3	FK WT	**1** (18.24)	**1** (36.22)	**1** (5.16)	**1** (6.89)	**1** (54.83)	**1** (489.78)
	FK p.E565A	**27** (490.91)	**42** (1,510.08)	**20** (105.68)	**5** (32.14)	**0.36** (19.72)	**4** (1,936.42)
	FK p.L617M	**126** (2,296.15)	**59** (2,152.78)	**28** (144.88)	**0.177** (1.22)	**14** (762.08)	**3** (1,674.94)
293T	FK WT	**1** (4.04)	**1** (7.80)	**1** (0.52)	**1** (1.35)	**1** (9.57)	**1** (161.81)
	FK p.E565A	**44** (176.39)	**84** (656.15)	**65** (33.65)	**11** (14.32)	**0.48** (4.55)	**8** (1,253.14)
	FK p.L617M	**12** (48.98)	**10** (76.74)	**31** (15.96)	**3** (4.59)	**0.40** (3.87)	**6** (990.83)
MMNK-1	FK WT	**1** (44.98)	**1** (4.08)	**1** (0.66)	**1** (0.20)	**1** (22.59)	**1** (77,983.01)
	FK p.E565A	**578** (26,001.60)	**257** (1,049.54)	**15** (10)	**Ambiguous** (>5,000)	**17** (387.26)	**0.03** (2,344.23)
	FK p.L617M	**213** (9,594.01)	**3** (10.69)	**17** (10.94)	**4** (0.74)	**2** (44.16)	**2151** (>5,000)

Note: Bold numbers represent fold change of inhibitor concentrations relative to FK WT. Nanomolar IC_{50} values are listed in parentheses for each inhibitor and condition. Values represent mean ± SEM of three independent experiments with six replicates per condition.

to other FGFR inhibitors seen in patients after FGFR inhibition (**Table 1**; Supplementary Fig. S2).

The presence of the *FGFR* p.E565A and p.L617M SNVs decreased sensitivity to FGFR inhibition, anywhere from 2- to 1,000-fold. Specifically, the p.L617M mutation demonstrated varying degrees of resistance depending on both the inhibitor and cell line used. The p.E565A mutation conferred the greatest degree of resistance across all cell lines and inhibitors tested. Furthermore, *FGFR2* p.E565A has been described previously as a recurrent acquired secondary resistance mutation in response to infigratinib therapy (16). However, the effect of this secondary resistance mutation on FGFR signaling has not been fully described.

Upregulation of PI3K/Akt/mTOR pathway in resistant cells

To characterize the signal transduction pathways involved in resistance to FGFR inhibition, we performed RPPA analysis on NIH3T3 empty, FK WT, and FK p.E565A cells. Using an FDR of 0.05, we identified proteins differentially expressed in FK WT compared with control cells and FK p.E565A compared with control cells (**Fig. 3A** and **B**). We identified that phosphorylated ribosomal protein S6 (RPS6) involved in PI3K/AKT/mTOR signaling was the most upregulated protein in FK WT (**Fig. 3A**) and FK p.E565A (**Fig. 3B**) cells relative to empty control. We next used STRING (30) to assess known and predicted protein–protein interactions within these differentially expressed protein sets. This analysis revealed activation of the PI3K/AKT signaling pathway in FK WT cells with an FDR of 0.00618 (**Fig. 3C**). In FK p.E565A cells, there was further potentiation of the PI3K/AKT pathway with an FDR of 1.96e-19 along with activation of the mTOR pathway with an FDR of 1.08e-17 (**Fig. 3D**). These findings were subsequently confirmed with Western blot analysis in NIH3T3 cells revealing upregulation of phospho-RPS6, phospho-AKT, and phospho-mTOR in both FK WT and FK p.E565A cells (**Fig. 3E**).

Treatment with the mTOR inhibitor, INK128, resensitizes resistant cells to FGFR inhibition

Having demonstrated upregulation of the PI3K/AKT/mTOR signaling pathway in FGFR-inhibitor–resistant FK p.E565A cells, we next sought to determine whether treatment with an mTOR inhibitor would enhance sensitivity to FGFR inhibitors. Sapanisertib (INK128, MLN0128, or TAK-228), is a highly potent, orally active mTOR kinase inhibitor that is currently in phase I and phase II clinical trials for solid tumors (31). We assessed the impact of INK128 on FGFR inhibitor (infigratinib, AZD4547, erdafitinib, or ponatinib) sensitivity (**Fig. 4A**). CalcuSyn was used to calculate a CI for each combination of drug concentrations (25 in total, **Fig. 4A**). On the basis of the CI value, the two drugs being evaluated were classified as synergistic (CI < 1), additive (CI = 1), or antagonistic (CI > 1). Combination of INK128 with all FGFR inhibitors demonstrated highly synergistic effects in FK p.E565A cells (**Fig. 4B**). We next extended these studies to cells harboring the second resistance mutation of interest, p.L617M, and found that combination of INK128 and FGFR inhibition yielded mildly synergistic effects (**Fig. 4B**). Average combination indexes for fraction affected (Fa) values greater than 0.1 are summarized in **Fig. 4C**. These data warrant further investigation of the addition of an mTOR inhibitor after initial progression with FGFR-targeted therapy.

Discussion

Through our case study of a patient with intrahepatic cholangiocarcinoma, we identified two *FGFR2* kinase domain mutations, p.E565A and p.L617M, associated with acquired resistance to the selective FGFR inhibitor infigratinib. Interestingly, only one of these mutations, *FGFR2* p.E565A, was identified through sequencing of a tumor biopsy collected from a progressing liver lesion; however, ctDNA captured this mutation as well as a second mutation, *FGFR2* p.L617M. These findings warrant further investigation into the use of ctDNA clinically to serially monitor early acquired resistance in patients receiving FGFR inhibitors. Using *in vitro* cell line models, we characterized the sensitivity of the FGFR2–KIAA1598 (FK) fusion with each of these secondary mutations to ATP-competitive, covalent, and nonselective FGFR inhibitors. Taken collectively, our findings suggest that these mutations confer resistance to FGFR inhibition, but remain sensitive to the nonselective FGFR inhibitor ponatinib. In addition, we identified the upregulation of the PI3K/AKT/mTOR signaling pathway in resistant cells and demonstrated that combining FGFR and mTOR inhibitors may be used to desensitize cells to FGFR resistance.

Tumor heterogeneity associated with acquired drug resistance remains a major barrier in the long-term clinical use of targeted therapies in patients with cancer (32). This heterogeneity includes but is not limited to differences in the genetic, epigenetic, and tumor microenvironment composition of tumors within the same tissue and between different tissue sites of the same patient (33–35). To date, the genomic evaluation of acquired drug resistance has been largely limited to tumor biopsies. Unfortunately, tumor biopsies pose several limitations including risk and cost to patients, restricted access to

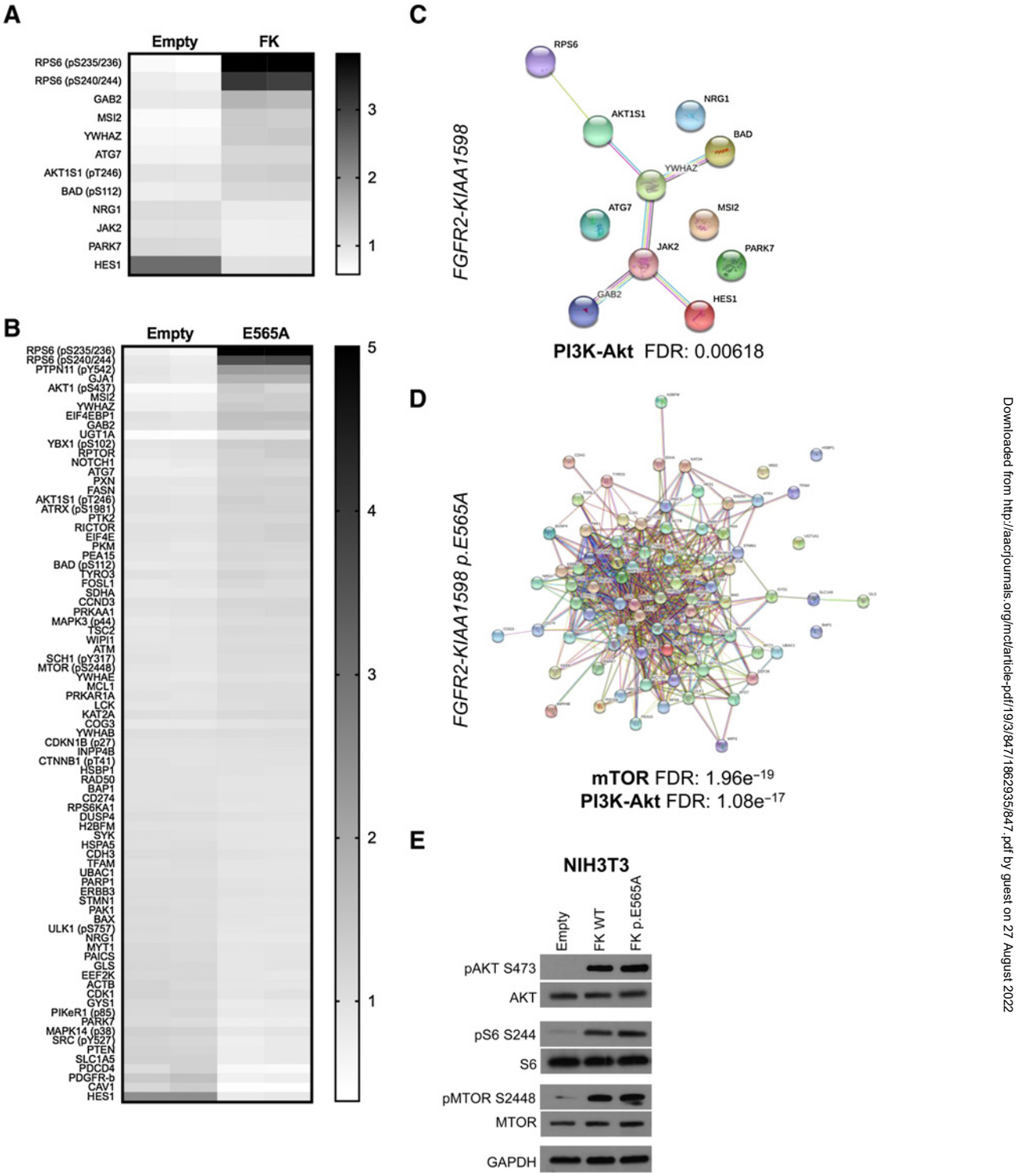

Figure 3.

The PI3K/AKT/mTOR signaling pathway is upregulated in fusion and resistant cells. **A,** Heatmap illustrates proteins from RPPA that were differentially expressed in FK WT relative to vector control (Empty) with an FDR of 0.05. **B,** Heatmap illustrates proteins from RPPA that were differentially expressed in FK p.E565A relative to vector control (Empty) with an FDR of 0.05. **C,** The STRING program was used to assess known and predicted protein–protein interactions within the differentially expressed proteins in FK WT cells. The PI3K/AKT pathway was identified with an FDR of 0.00618. **D,** The STRING program was used to assess known and predicted protein–protein interactions within the differentially expressed proteins in FK p.E565A cells. The PI3K/AKT pathway and mTOR pathways were identified with FDRs of 1.96e-19 and of 1.08e-17, respectively. **E,** Western blot analysis to confirm RPPA data in NIH3T3 cells.

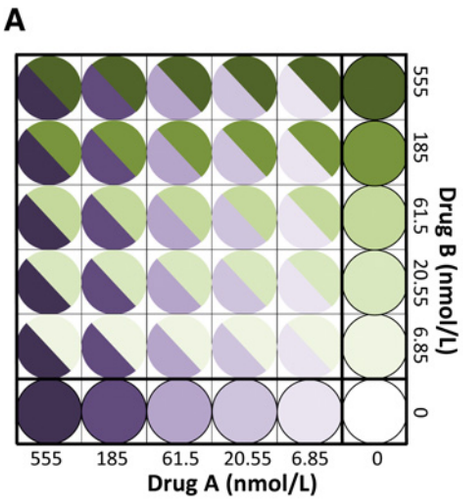

C

	Combination index (SD)	
	p.E565A	p.L617M
Infigratinib	0.44 (0.21)	0.88 (0.48)
AZD-4547	0.98 (0.91)	1.08 (0.94)
Erdafitinib	0.53 (0.44)	1.10 (0.55)
Ponatinib	0.53 (0.29)	1.09 (0.48)

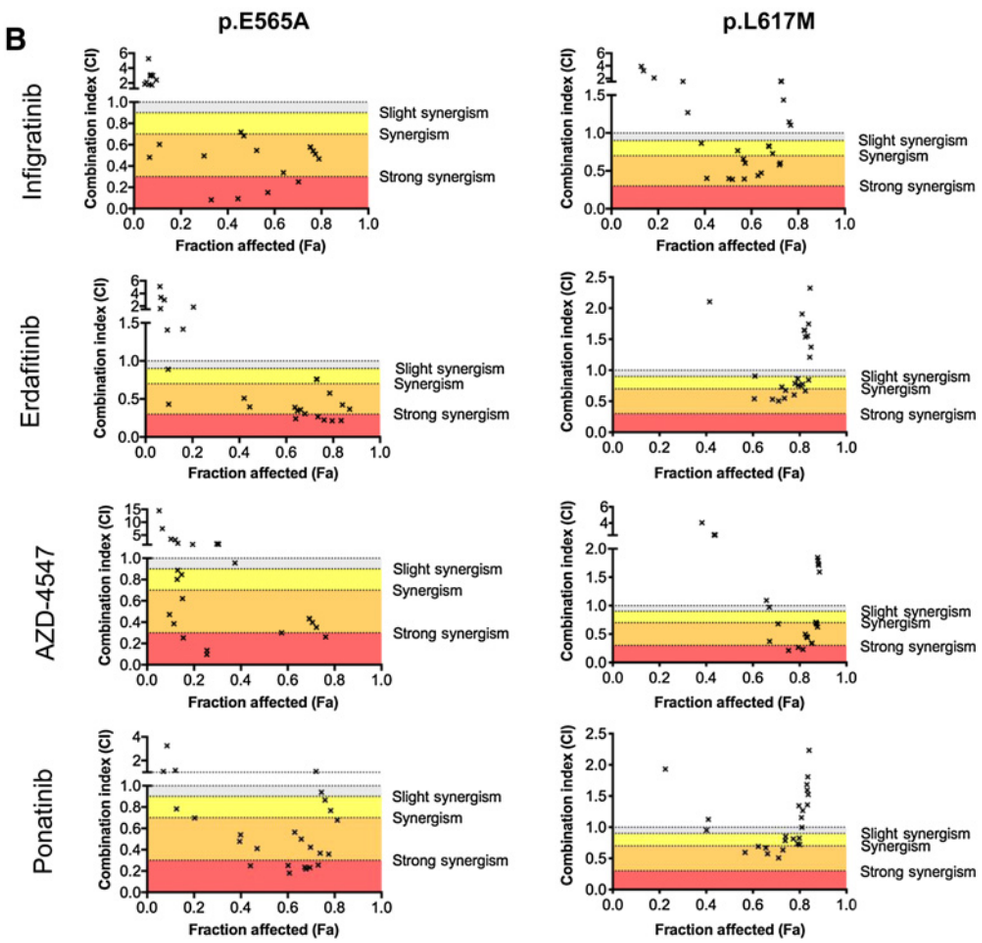

Figure 4.

Combination of FGFR inhibitors with the mTOR inhibitor, INK128, reveals synergistic effects in resistant cell lines. **A,** Experimental design for drug combination assays. **A**. In duplicate in a 96-well plate, cells were exposed to either drug A, drug B, drug A plus drug B, or no drug control with concentrations of drugs from 6.85 nmol/L to 555 nmol/L. **B,** CI and Fa for each combination drug value are plotted. Values are defined as displaying slight synergism, synergism, or strong synergism. Graphs depict summary data from four independent experiments for infigratinib, AZD-4547, erdafitinib, and ponatinib. **C,** Average CI values are listed for drug combinations that had Fa values greater than 0.1. SD values from four independent experiments are listed in parentheses. CI, combination index; Fa, fraction affected.

certain organs/tissue sites, finite amounts of tissue collected, and sampling from only one tissue site at a single time point. Furthermore, tumor biopsies do not accurately portray the complex and complete genetic profile of disease. ctDNA has the potential to fully capture tumor heterogeneity including the presence of acquired secondary resistance mutations in patients receiving targeted therapies and therefore has the potential to overcome limitations associated with tumor biopsies. Importantly, in 80%–90% of patients with metastatic disease, ctDNA can accurately reconstruct the genome with a high mutational concordance to matched tumor tissues (36–39). In contrast to this high mutational concordance between matched tissues and ctDNA, studies have recently shown that tumor biopsies are inaccurate at fully describing the landscape of acquired secondary resistance mutations following FGFR inhibition. In a recent publication by Goyal and colleagues, the authors demonstrated that ctDNA can identify FGFR*2* mutations that were not present in the tumor biopsies from the same patient (16). Furthermore, in the patient presented in this study, the *FGFR2* p.L617M mutation was identified in ctDNA but was not detected in the tissue biopsy specimen. Collectively, these findings highlight the inter- and intratumor heterogeneity that exists within patients. ctDNA is less invasive, can be collected serially, and thus may be a clinically useful method to track tumor heterogeneity with respect to acquired FGFR resistance mutations in patients. Moving forward, upon progression we propose a combination of tumor biopsy and ctDNA for patients with FGFR-mutant cancers. This will enable a complementary view of genomic changes (ctDNA) as well as transcriptomic and protein level alterations (biopsy) in resistant tumors.

As the continuously evolving landscape of clinically relevant nonselective and selective FGFR inhibitors expands, it is critical to catalog these inhibitors based on their effectiveness against acquired secondary resistance mutations. Dovitinib, ponatinib, and lenvatinib are nonselective TKIs that in addition to FGFR, target multiple other receptor tyrosine kinases, including VEGFR and PDGFR (40–42). Interestingly, our *in vitro* studies support the use of ponatinib following acquisition of both the p.E565A and p.L617M secondary mutations as they retained sensitivity to ponatinib at nanomolar concentrations. Unfortunately, given the nonselective activity of these inhibitors, severe cardiovascular toxicities related to VEGFR inhibition have been seen in patients therefore limiting their long-term clinical use (43). Thus, there has been great interest in the development of selective FGFR inhibitors. Currently, numerous selective ATP-competitive FGFR inhibitors are being assessed clinically including AZD4547, infigratinib, erdafitinib, pemigatinib (INCB054828), and LY2874455, among others (12, 44, 45). While these inhibitors have shown promising activity in early clinical trials, they are largely ineffective at overcoming the commonly acquired FGFR gatekeeper mutations (*FGFR1* V561M, *FGFR2* V564F, *FGFR3* V555M). While not considered gatekeeper mutations, the *FGFR2* p.E565A and *FGFR2* p.L617M mutations we observed are located near the ATP-binding pocket and are hypothesized to also be resistant to these selective inhibitors. Our studies revealed cross-resistance to all selective inhibitors tested; however, the level of resistance observed varied across the different drugs. There has been great interest in developing novel inhibitors that can overcome resistance mutations that arise in or near the ATP-binding pocket. One such inhibitor is TAS120, which retained activity in the presence of either mutation in our *in vitro* assays. to which the two mutations in our studies largely still retained sensitivity. Taken together, there is a need to define a comprehensive landscape of mutations that develop in response to FGFR inhibition, including the sensitivity of existing inhibitors to develop novel inhibitors.

In addition to acquired *FGFR2* mutations, numerous studies have identified activation of the PI3K/AKT/mTOR pathway following acquired resistance to FGFR inhibition. Through RPPA analysis, we also identified increased PI3K/AKT/mTOR activation in an FGFR inhibitor–resistant cell line and determined that combination therapy using an FGFR inhibitor with the mTOR inhibitor, INK128, was able to induce synergistic effects that may be able to overcome the therapeutic limitations posed by current mechanisms of resistance. Similarly, Hu and colleagues found that antiproliferative effects were increased in FGFR-addicted cells after treatment with a combination of infigratinib and another mTOR inhibitor, rapamycin (46). In addition, a recent study by Scheller and colleagues provides evidence for the combination of FGFR and mTOR inhibition in hepatocellular carcinoma (47). This concept has been expanded beyond FGFR inhibition as demonstrated by Baselga and colleagues who showed that in hormone receptor–positive breast cancer, the PI3K/AKT/mTOR pathway was implicated in therapy resistance (48). As a result, the combination therapy of exemestane, a steroidal aromatase inhibitor and everolimus, an mTOR inhibitor, was approved for clinical use (49). These studies support the idea that drug combination strategies involving common bypass resistance mechanisms could provide a novel therapeutic avenue to patients who have exhibited resistance to an existing FGFR inhibitor while we wait the development of novel FGFR inhibitors.

Overall, our findings support the complementary use of a repeat tumor biopsy upon progression coupled with serial ctDNA analysis throughout treatment to characterize emerging resistance mechanisms in FGFR-altered cancers. Understanding genetic and proteomic alterations will enable the rational implementation of novel combination therapeutic strategies in addition to development of novel FGFR inhibitors to overcome acquired resistance.

Disclosure of Potential Conflicts of Interest

H.-Z. Chen reports receiving speakers bureau honoraria from QED. K.K. Ciombor reports receiving commercial research grant from Incyte. S. Roychowdhury is an employee/paid consultant for Incyte Pharm, QED Therapeutics, and AbbVie; reports receiving commercial research grants from Incyte Pharm and QED Therapeutics; and reports receiving speakers bureau honoraria from IDT Technologies. No potential conflicts of interest were disclosed by the other authors.

Authors' Contributions

Conception and design: M.A. Krook, J. Hays, S. Roychowdhury
Development of methodology: M.A. Krook, M. Dantuono, H.-Z. Chen, D.M. Martin
Acquisition of data (provided animals, acquired and managed patients, provided facilities, etc.): M.A. Krook, A. Lenyo, H. Barker, K.M. Bailey, J.W. Reeser, A.M. Smith, T. Dao, K.K. Ciombor
Analysis and interpretation of data (e.g., statistical analysis, biostatistics, computational analysis): M.A. Krook, A. Lenyo, M. Wilberding, H. Barker, M. Dantuono, H.-Z. Chen, M.R. Wing, J. Miya, E. Samorodnitsky, A.M. Smith, J. Hays, A.G. Freud, S. Roychowdhury
Writing, review, and/or revision of the manuscript: M.A. Krook, A. Lenyo, M. Wilberding, K.M. Bailey, H.-Z. Chen, J.W. Reeser, M.R. Wing, E. Samorodnitsky, K.K. Ciombor, J. Hays, A.G. Freud, S. Roychowdhury
Administrative, technical, or material support (i.e., reporting or organizing data, constructing databases): M.A. Krook, D.M. Martin, J. Hays
Study supervision: M.A. Krook, S. Roychowdhury

Acknowledgments

The authors would like to first and foremost thank the patient and her family. The authors would also like to thank Jenny Badillo for her administrative support; the Ohio State University Comprehensive Cancer Center, community philanthropic support, Pelotonia; the Ohio Supercomputer Center for providing the resources necessary for bioinformatics analysis; and current and past members of the Roychowdhury lab. S. Roychowdhury was supported by an American Cancer Society grant MRSG-12-194-01-TBG, NCI UH2CA202971 (SpARKFuse), NCI UH2CA216432 (MSIDx), and Pelotonia. M.A. Krook is supported by a T32 Oncology

Training Grant (5T32CA009338) and Award Number Grant TL1TR002735 from the National Center for Advancing Translational Sciences. A. Lenyo and M. Wilberding were supported by a Pelotonia Undergraduate Research Fellowship. K.M. Bailey is supported by an Alex's Lemonade Stand Young Investigator Award, Children's Cancer Research Fund Emerging Scientist Grant, NIHK12 (2K12HD052892-11A1). H.Z. Chen is supported by a Pelotonia Post-Doctoral Research Fellowship and American Society of Clinical Oncology Young Investigator Award.

The costs of publication of this article were defrayed in part by the payment of page charges. This article must therefore be hereby marked *advertisement* in accordance with 18 U.S.C. Section 1734 solely to indicate this fact.

Received June 25, 2019; revised October 15, 2019; accepted December 19, 2019; published first January 7, 2020.

References

1. PDQ Adult Treatment Editorial Board. Bile duct cancer (cholangiocarcinoma) treatment (PDQ®): health professional version. PDQ cancer information summaries. Bethesda, MD: National Cancer Institute; 2002.
2. Razumilava N, Gores GJ. Cholangiocarcinoma. Lancet 2014;383:2168–79.
3. Javle M, Lowery M, Shroff RT, Weiss KH, Springfeld C, Borad MJ, et al. Phase II study of BGJ398 in patients with FGFR-altered advanced cholangiocarcinoma. J Clin Oncol 2018;36:276–82.
4. Jain A, Borad MJ, Kelley RK, Wang Y, Abdel-Wahab R, Meric-Bernstam F, et al. Cholangiocarcinoma with FGFR genetic aberrations: a unique clinical phenotype. JCO Precis Oncol 2018:1–12.
5. Borad MJ, Davis SL, Lowery MA, Lihou CF, Abou-Alfa GK. Phase 2, open-label, multicenter study of the efficacy and safety of INCB054828 in patients (pts) with advanced, metastatic, or surgically unresectable cholangiocarcinoma (CCA) with inadequate response to prior therapy. J Clin Oncol 35:15s, 2017 (suppl; abstr TPS4145).
6. Wu YM, Su F, Kalyana-Sundaram S, Khazanov N, Ateeq B, Cao X, et al. Identification of targetable FGFR gene fusions in diverse cancers. Cancer Discov 2013;3:636–47.
7. Turner N, Grose R. Fibroblast growth factor signalling: from development to cancer. Nat Rev Cancer 2010;10:116–29.
8. Helsten T, Elkin S, Arthur E, Tomson BN, Carter J, Kurzrock R. The FGFR landscape in cancer: analysis of 4,853 tumors by next-generation sequencing. Clin Cancer Res 2016;22:259–67.
9. Touat M, Ileana E, Postel-Vinay S, Andre F, Soria JC. Targeting FGFR signaling in cancer. Clin Cancer Res 2015;21:2684–94.
10. Holzmann K, Grunt T, Heinzle C, Sampl S, Steinhoff H, Reichmann N, et al. Alternative splicing of fibroblast growth factor receptor IgIII loops in cancer. J Nucleic Acids 2012;2012:950508.
11. Wendt MK, Taylor MA, Schiemann BJ, Sossey-Alaoui K, Schiemann WP. Fibroblast growth factor receptor splice variants are stable markers of oncogenic transforming growth factor beta1 signaling in metastatic breast cancers. Breast Cancer Res 2014;16:R24.
12. Chae YK, Ranganath K, Hammerman PS, Vaklavas C, Mohindra N, Kalyan A, et al. Inhibition of the fibroblast growth factor receptor (FGFR) pathway: the current landscape and barriers to clinical application. Oncotarget 2017;8:16052–74.
13. Branford S, Rudzki Z, Walsh S, Parkinson I, Grigg A, Szer J, et al. Detection of BCR-ABL mutations in patients with CML treated with imatinib is virtually always accompanied by clinical resistance, and mutations in the ATP phosphate-binding loop (P-loop) are associated with a poor prognosis. Blood 2003;102:276–83.
14. Roberts KG, Odell AF, Byrnes EM, Baleato RM, Griffith R, Lyons AB, et al. Resistance to c-KIT kinase inhibitors conferred by V654A mutation. Mol Cancer Ther 2007;6:1159–66.
15. Gazdar AF. Activating and resistance mutations of EGFR in non-small-cell lung cancer: role in clinical response to EGFR tyrosine kinase inhibitors. Oncogene 2009;28:S24–31.
16. Goyal L, Saha SK, Liu LY, Siravegna G, Leshchiner I, Ahronian LG, et al. Polyclonal secondary FGFR2 mutations drive acquired resistance to FGFR inhibition in patients with FGFR2 fusion-positive cholangiocarcinoma. Cancer Discov 2017;7:252–63.
17. Goyal L, Shi L, Liu LY, Fece de la Cruz F, Lennerz JK, Raghavan S, et al. TAS-120 overcomes resistance to ATP-competitive FGFR inhibitors in patients with FGFR2 fusion-positive intrahepatic cholangiocarcinoma. Cancer Discov 2019;9:1064–79.
18. Reeser JW, Martin D, Miya J, Kautto EA, Lyon E, Zhu E, et al. Validation of a targeted RNA sequencing assay for kinase fusion detection in solid tumors. J Mol Diagn 2017;19:682–96.
19. Samorodnitsky E, Datta J, Jewell BM, Hagopian R, Miya J, Wing MR, et al. Comparison of custom capture for targeted next-generation DNA sequencing. J Mol Diagn 2015;17:64–75.
20. Reid Y, Storts D, Riss T, Minor L. Authentication of human cell lines by STR DNA profiling analysis. In: Sittampalam GS, Coussens NP, Brimacombe K, Grossman A, Arkin M, Auld D, et al. , editors. Assay guidance manual. Bethesda, MD: Eli Lilly & Company and the National Center for Advancing Translational Sciences; 2004.
21. Krook MA, Barker H, Chen HZ, Reeser JW, Wing MR, Martin D, et al. Characterization of a KLK2-FGFR2 fusion gene in two cases of metastatic prostate cancer. Prostate Cancer Prostatic Dis 2019;22:624–32.
22. Liu J, Peng X, Dai Y, Zhang W, Ren S, Ai J, et al. Design, synthesis and biological evaluation of novel FGFR inhibitors bearing an indazole scaffold. Org Biomol Chem 2015;13:7643–54.
23. Kalyukina M, Yosaatmadja Y, Middleditch MJ, Patterson AV, Smaill JB, Squire CJ. TAS-120 cancer target binding: defining reactivity and revealing the first fibroblast growth factor receptor 1 (FGFR1) irreversible structure. ChemMedChem 2019;14:494–500.
24. Szklarczyk D, Franceschini A, Wyder S, Forslund K, Heller D, Huerta-Cepas J, et al. STRING v10: protein-protein interaction networks, integrated over the tree of life. Nucleic Acids Res 2015;43:D447–52.
25. Fraser C, Carragher NO, Unciti-Broceta A. eCF309: a potent, selective and cell-permeable mTOR inhibitor. MedChemComm 2016;7:471–7.
26. Chou TC. Drug combination studies and their synergy quantification using the Chou-Talalay method. Cancer Res 2010;70:440–6.
27. Datta J, Damodaran S, Parks H, Ocrainiciuc C, Miya J, Yu L, et al. Akt activation mediates acquired resistance to fibroblast growth factor receptor inhibitor BGJ398. Mol Cancer Ther 2017;16:614–24.
28. Maruyama M, Kobayashi N, Westerman KA, Sakaguchi M, Allain JE, Totsugawa T, et al. Establishment of a highly differentiated immortalized human cholangiocyte cell line with SV40T and hTERT. Transplantation 2004;77:446–51.
29. Toriyama M, Shimada T, Kim KB, Mitsuba M, Nomura E, Katsuta K, et al. Shootin1: a protein involved in the organization of an asymmetric signal for neuronal polarization. J Cell Biol 2006;175:147–57.
30. Szklarczyk D, Morris JH, Cook H, Kuhn M, Wyder S, Simonovic M, et al. The STRING database in 2017: quality-controlled protein-protein association networks, made broadly accessible. Nucleic Acids Res 2017;45:D362–D8.
31. Moore KN, Bauer TM, Falchook GS, Chowdhury S, Patel C, Neuwirth R, et al. Phase I study of the investigational oral mTORC1/2 inhibitor sapanisertib (TAK-228): tolerability and food effects of a milled formulation in patients with advanced solid tumours. ESMO Open 2018;3:e000291.
32. Holohan C, Van Schaeybroeck S, Longley DB, Johnston PG. Cancer drug resistance: an evolving paradigm. Nat Rev Cancer 2013;13:714–26.
33. Meacham CE, Morrison SJ. Tumour heterogeneity and cancer cell plasticity. Nature 2013;501:328–37.
34. Junttila MR, de Sauvage FJ. Influence of tumour micro-environment heterogeneity on therapeutic response. Nature 2013;501:346–54.
35. Heng HH, Bremer SW, Stevens JB, Ye KJ, Liu G, Ye CJ. Genetic and epigenetic heterogeneity in cancer: a genome-centric perspective. J Cell Physiol 2009;220:538–47.
36. Yong E. Cancer biomarkers: written in blood. Nature 2014;511:524–6.
37. Lanman RB, Mortimer SA, Zill OA, Sebisanovic D, Lopez R, Blau S, et al. Analytical and clinical validation of a digital sequencing panel for quantitative, highly accurate evaluation of cell-free circulating tumor DNA. PLoS One 2015;10:e0140712.
38. Bettegowda C, Sausen M, Leary RJ, Kinde I, Wang Y, Agrawal N, et al. Detection of circulating tumor DNA in early- and late-stage human malignancies. Sci Transl Med 2014;6:224ra24.

39. Zill OA, Greene C, Sebisanovic D, Siew LM, Leng J, Vu M, et al. Cell-free DNA next-generation sequencing in pancreatobiliary carcinomas. Cancer Discov 2015;5:1040–8.
40. Sarker D, Molife R, Evans TR, Hardie M, Marriott C, Butzberger-Zimmerli P, et al. A phase I pharmacokinetic and pharmacodynamic study of TKI258, an oral, multitargeted receptor tyrosine kinase inhibitor in patients with advanced solid tumors. Clin Cancer Res 2008;14:2075–81.
41. Gozgit JM, Wong MJ, Moran L, Wardwell S, Mohemmad QK, Narasimhan NI, et al. Ponatinib (AP24534), a multitargeted pan-FGFR inhibitor with activity in multiple FGFR-amplified or mutated cancer models. Mol Cancer Ther 2012;11: 690–9.
42. Matsui J, Yamamoto Y, Funahashi Y, Tsuruoka A, Watanabe T, Wakabayashi T, et al. E7080, a novel inhibitor that targets multiple kinases, has potent antitumor activities against stem cell factor producing human small cell lung cancer H146, based on angiogenesis inhibition. Int J Cancer 2008;122:664–71.
43. Gagnieu MC, Heiblig M, Blond E, Legros L, Guillermin Y, Morisset S, et al. Cardiovascular events occurring on ponatinib in chronic phase chronic myeloid leukemia patients, preliminary analysis of a multicenter cohort. Blood 2013; 122:4020.
44. Michael M, Bang YJ, Park YS, Kang YK, Kim TM, Hamid O, et al. A phase 1 study of LY2874455, an oral selective pan-FGFR inhibitor, in patients with advanced cancer. Targeted Oncol 2017;12:463–74.
45. Saleh M, Gutierrez ME, Subbiah V, Smith DC, Asatiani E, Lihou CF, et al. Preliminary results from a phase 1/2 study of INCB054828, a highly selective fibroblast growth factor receptor (FGFR) inhibitor, in patients with advanced malignancies [abstract]. In: Proceedings of the American Association for Cancer Research Annual Meeting 2017; 2017 Apr 1–5; Washington, DC. Philadelphia (PA): AACR; 2017. Abstract nr CT111.
46. Hu Y, Lu H, Zhang J, Chen J, Chai Z, Zhang J. Essential role of AKT in tumor cells addicted to FGFR. Anticancer Drugs 2014;25:183–8.
47. Scheller T, Hellerbrand C, Moser C, Schmidt K, Kroemer A, Brunner SM, et al. mTOR inhibition improves fibroblast growth factor receptor targeting in hepatocellular carcinoma. Br J Cancer 2015;112:841–50.
48. Baselga J, Campone M, Piccart M, Burris HA 3rd, Rugo HS, Sahmoud T, et al. Everolimus in postmenopausal hormone-receptor-positive advanced breast cancer. N Engl J Med 2012;366:520–9.
49. Royce ME, Osman D. Everolimus in the treatment of metastatic breast cancer. Breast Cancer 2015;9:73–9.